LAWRENCE
LIVERMORE
NATIONAL
LABORATORY

UCRL-PROC-212752

Interpretation Of Multifrequency Crosswell Electromagnetic Data With Frequency Dependent Core Data

Barry Kirkendall, Jeffery Roberts

June 7, 2005

2nd International Rainbow in the Earth Workshop: Frequency-Dependent Geophysical Properties and Their Relationships to Rock Properties at Multiple Scales
Berkeley, CA, United States
August 7, 2005 through August 18, 2005

PROCEEDINGS, Rainbow in the Earth – 2nd International Workshop 2005
Lawrence Berkeley National Laboratory, Berkeley, California, August 17-18, 2005

Interpretation Of Multifrequency Crosswell Electromagnetic Data With Frequency Dependent Core Data

Barry Kirkendall
Jeffery J. Roberts

Lawrence Livermore National Laboratory
7000 East Avenue L-206
Livermore, CA 94550 USA
e-mail: Kirkendall1@llnl.gov, Roberts17@llnl.gov

ABSTRACT

Interpretation of cross-borehole electromagnetic (EM) images acquired at enhanced oil recovery (EOR) sites has proven to be difficult due to the typically complex subsurface geology. Significant problems in image interpretation include correlation of specific electrical conductivity values with oil saturations, the time-dependent electrical variation of the subsurface during EOR, and the non-unique electrical conductivity relationship with subsurface conditions. In this study we perform laboratory electrical properties measurements of core samples from the EOR site to develop an interpretation approach that combines field images and petrophysical results. Cross-borehole EM images from the field indicate resistivity increases in EOR areas—behavior contrary to the intended waterflooding design. Laboratory measurements clearly show a decrease in resistivity with increasing effective pressure and are attributed to increased grain-to-grain contact enhancing a strong surface conductance. We also observe a resistivity increase for some samples during brine injection. These observations possibly explain the contrary behavior observed in the field images. Possible mechanisms for increasing the resistivity in the region include (1) increased oil content as injectate sweeps oil toward the plane of the observation wells; (2) lower conductance pore fluid displacing the high-conductivity brine; (3) degradation of grain-to-grain contacts of the initially conductive matrix; and (4) artifacts of the complicated resistivity/time history similar to that observed in the laboratory experiments.

INTRODUCTION

Electromagnetic methods are highly sensitive to the amount, state, and composition of subsurface fluids, while seismic methods provide information concerning subsurface structure. Borehole EM techniques can be applied to characterize subsurface resources and to monitoring production and resource recovery processes in the oil field because of the subsurface fluid information provided by EM responses. These techniques have numerous applications including the focus of this paper, enhanced oil recovery (EOR). The technique of cross-borehole EM induction uses kilohertz-frequency EM fields to image the electrical conductivity structure in the plane intersecting two boreholes through geophysical inversion. Recent efforts to study and increase borehole EM field and processing resolution [*Alumbaugh and Newman*, 2000], borehole EM inversion algorithm efficiency [*Newman and Alumbaugh*, 1997; *Newman*, 1995], and borehole ambient noise sources [*Zhu et al*., 1999] have resulted in advances in inverting data into pseudo-images. However, the interpretation of these pseudo-images remains undeveloped.

Using cross-borehole EM induction imaging, we attempt to improve interpretation techniques by incorporating petrophysical analysis from core samples, formation fluids, and injection fluids obtained from the site. We account for resistivity values in samples saturated with both formation fluid and injection fluid, determine the volume of oil moved through the sample during brine injection, and provide information on resistivity as a function of injection time for the core samples. We develop a qualitative interpretation approach that uses field images and petrophysical results from laboratory analyses to assign accurate conductivity values for inversion images and to gain a clearer picture of the extent and effectiveness of EOR using water injection.

The site under investigation, defined as a heavy oil reservoir producing with an API index of 17, consists predominantly of high-porosity and extremely-low-permeability diatomaceous deposits. EOR in the area has proven somewhat ineffective because fracture-induced injection flow dominates matrix flow. The ability to rapidly image the flow of water injection is therefore crucial to optimizing EOR and understanding the subsurface system. The purpose of this paper is to report field and laboratory results for an active, well-characterized EOR site and to demonstrate that interpretations that include analysis and consideration of physical properties determined by borehole and laboratory methods help obtain more in-depth understanding of injection and EOR processes. These methods can be applied to an arbitrary site.

LABORATORY EXPERIMENT

Electrical Measurements

A four-terminal pair, two-electrode lead configuration was used to measure the complex impedance as a function of frequency. Data were taken with an HP 4284A LCR meter. All instruments are high-input impedance devices that measure impedance magnitude |Z|, phase angle f, resistance R, and capacitance C. The error of measurement varies according to frequency and resistance, but is generally less than 1% up to 100 kΩ, and within 5% at the highest impedance limits (>100 MW). The system was periodically checked for accuracy using a set of 1% tolerance resistors and capacitors and was found to yield consistent values.

Laboratory Procedures

Laboratory electrical measurements were performed at temperatures up to 50°C with separate confining and pore pressure control. The experimental apparatus consists of an externally heated pressure vessel with separate pumps and controls for confining pressure and pore pressure on either side of the sample. Pore pressure was controlled independently between 0.1 and 3.7 MPa, and for convenience the two systems are referred to as up- and down-stream pressure systems. The impedance bridge (HP 4284A) was used to continuously measure the resistance of the electrically isolated samples at 0.1, 1.0, and 10 kHz. Electrical resistivity was calculated from the resistance and geometry of the core. Calibration runs using Teflon blanks showed no current leakage through alternate electrical pathways.

FIELD EXPERIMENT

Experiment Description

The technique of cross-borehole electromagnetic imaging, described in *Wilt et al.* [1995], is analogous to the technique of seismic borehole tomography [*Ivansson*, 1986; *Gustavsson*, 1986]. One specific difference is that EM induction continuously operates in the frequency domain with a kilohertz-frequency source signal. Keeping the vertical dipole receiver antenna stationary and moving the vertical dipole transmitter antenna through the depth section of interest, we record the total field which consists of the scattered and directly arrived energy. A digital phase-lock loop with amplification isolates the signal by using a fiber-optic cable to transmit the instantaneous transmitter frequency. The total field is stacked for 300 ms, line-filtered before isolation, and sampled from the phase lock loop output at 1.0 Hz; this provides a stable data point approximately every 0.10 m assuming an infinitesimally small transmitter and receiver

Field Data Discussion

Figure 1 shows two-dimensional electrical conductivity pseudo-images acquired in April 2001 at 2.0 kHz (top) and 6.0 kHz (bottom) source frequencies. This image clearly shows the locations of higher oil (higher resistivity shown by yellow hue) and brine concentrations (lower resistivity shown by blue hue). Contrasting depth intervals of this image are in between 540 and 555 meters, where

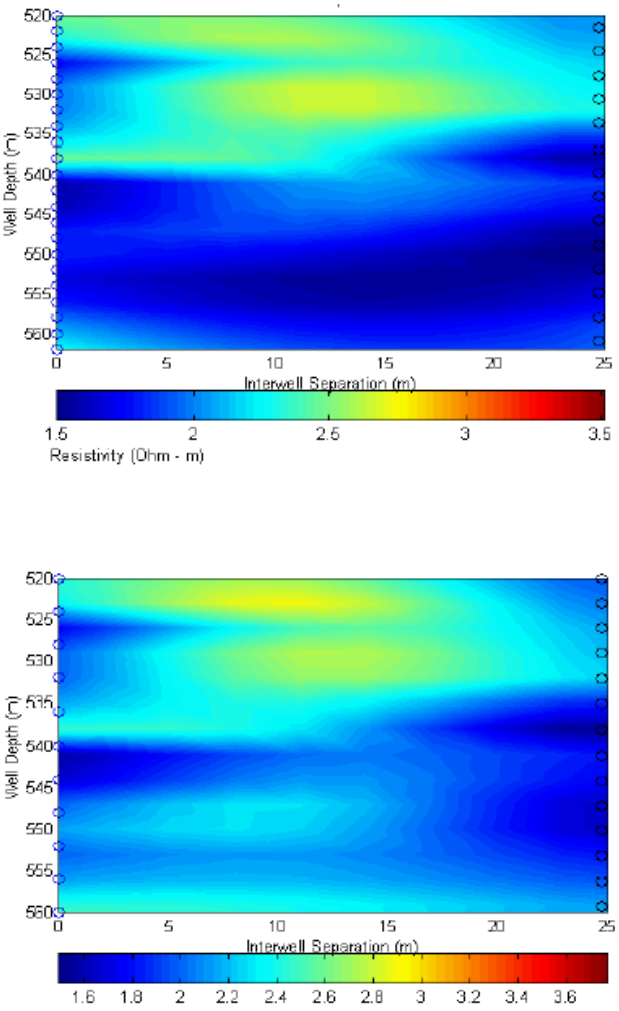

Figure 1. Crosswell EMIT pseudo-images acquired at different frequencies; 2.0 kHz (top) and 6.0 kHz (below) These images were inverted using with a FDFD code developed at SNL and LBNL.

data would suggest differing results. A calculation of the effect of the two frequencies on the induction number indicate that the frequency difference should be much less than shown in Figure 1. Therefore, the difference is either due to inversion or data acquisition error or frequency dependence of the

fluids. The true situation is likely the latter. In the upper region, water injection has clearly swept the oil deposits, although in the lower region, EOR has not been effective. Permeability logs suggest that the reason for this decrease in water movement is simply the increase in permeability, also shown in core samples. Additionally, the majority of small-scale flow as indicated by petrophysical measurements is through the rock matrix. As diatomite can be considered an unconsolidated formation, small-scale fractures do not contribute toward significant amounts of flow. Hydraulic fracturing, however, is a cause of large-scale fracture flow, and this large-scale flow may be contributing to a significant volume of water leaving the injection area.

RESULTS

Laboratory Results

Electrical resistivity during brine injection

Once the samples were at pressure and oil-saturated, the resistivity was monitored while brine was forced through the sample. One such result is shown in Figure 2, where resistivity is plotted as a function of time. For each sample a relatively constant oil-saturated resistivity was established followed by the injection of brine as indicated by the vertical dashed line. The confining pressure and pore-pressure

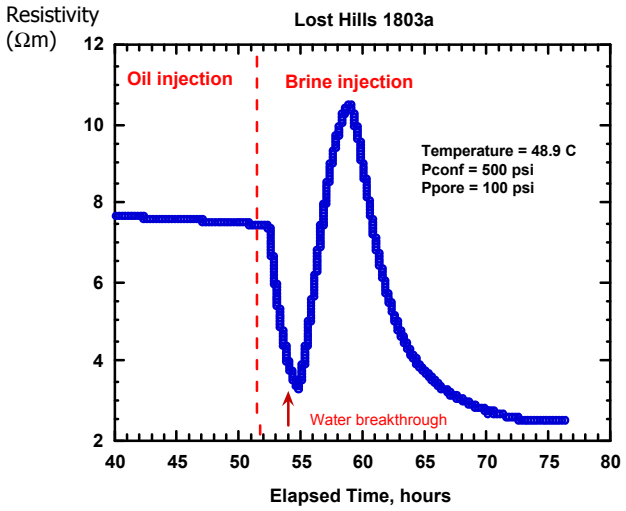

Figure 2. Electrical resistivity measured at 1 kHz as a function of time for a core. Sample, temperature, and confining and pore pressure of each run is listed on the individual plot. The vertical red-dashed line on each plot marks the change from oil to brine injection. The peak at 55 hours is unexpected and discussed in text.

gradient were typically 3.4 and1.7 MPa, respectively, but both were higher for relatively impermeable samples. For all samples the final brine-filled resistivity value is lower than the initial oil-filled resistivity and the ratio of oil- to brine-saturated resistivity ranges between 1.8 and 6.7 and does not appear to correlate with either porosity or permeability as reported by our industrial partner.

Electrical resistivity as a function of pressure

The resistivity as a function of effective pressure (confining pressure–pore pressure) will be discussed in the talk but are not shown here. These measurements were performed at the beginning of each sample run prior to heating. All samples displayed a similar behavior: decreasing resistivity with increasing effective (or confining) pressure. This trend is in conflict with the result of Walsh and Brace (1984) where an increase in confining pressure caused an increase in the resistivity of most porous rocks studied. Possible reasons for this behavior include the presence of a solid state conduction mechanism (as opposed to an electrolytic conduction mechanism), such as a conducting film or conductive mineral phase, that is more conducting with better grain-to-grain contact as pressure is applied. Another possibility is that increasing the confining pressure crushes the sample, thereby increasing the permeability as well as enhancing electrical transport. Post-run sample characterization via optical and electron microscopy did not provide convincing evidence for one explanation over another.

Frequency dependence of impedance measurements

At several times during the core injection process, a network analyzer was used to measure the impedance response as a function of frequency. Figure 3 shows

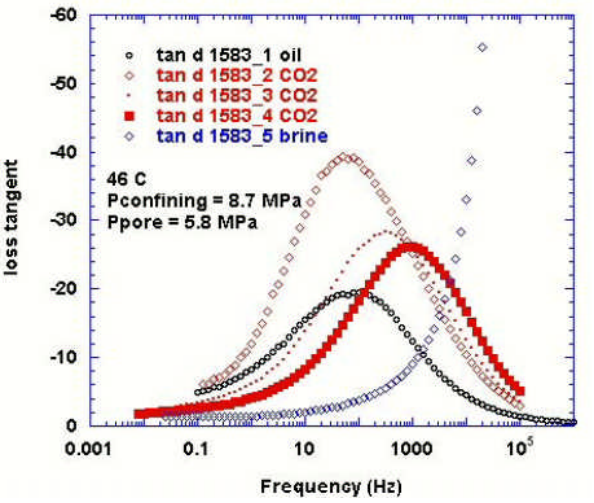

Figure 3. Initial impedance measurements of core indicate changing loss tangent response as a function of frequency with saturating oil, CO_2, and brine.

the results and is the basis for our multi-frequency measurements in the field data. Clearly, the magnitude and phase each have distinct frequency ranges where the oil and brine (and CO2 for reference) can best be distinguished. We discuss these relationships to field data in our talk.

DISCUSSION

The expected behavior is that as the injected water displaces the non-conducting oil, the resistivity will decrease. At first glance we observe that resistivity does not change uniformly with water injection. Another complicating factor is the difference in electrical resistivity of the produced versus injected water.

The cross-well EM induction pseudo-image taken November 1999 is in general agreement with the induction logs from August 1999 (Figure 1). This snapshot images occurred over a period of time with continuous water injection. At these depths between the observation wells we might expect the most changes in resistivity. However, the largest resistivity change is positive, toward more resistive pore fluids and slightly offset from the injector horizons. The question is, what does this resistivity increase represent?

Possible mechanisms for increasing the resistivity in this region include (1) increased oil content as injectate sweeps oil toward the plane of the observation wells; (2) lower-conductance pore fluid displacing the high-conductivity brine; (3) degradation of grain-to-grain contacts of the initially conductive matrix; and (4) artifact of the complicated resistivity/time history similar to that observed in the lab experiments.

The first mechanism, increased oil content due to EOR, can possibly be checked by examining production history of nearby wells. The second mechanism, changing pore fluid conductivity, is reasonable because the highest observed resistivity change is slightly less than 1 W-m and the different fluids have a difference in resistivity of about 0.6 W-m. But, since the change is larger than this in at least some portion of the image plane, an additional or combination of mechanisms is likely. The third and fourth explanations are similar in that both involve some conduction mechanism other than aqueous conduction through fluid-filled pores. A resistivity anomaly consistent with solid-state conduction was clearly observed in the laboratory experimental results as evidenced by the resistivity dependence on effective pressure and the resistivity increase for some samples during brine injection.

One observation we can make is that the anomalous increase in resistivity occurs at earliest times for the samples with the highest permeability. This complicates the interpretation of both well induction logs and the field images because different samples display different time-dependent resistivity changes, and we don't expect equal injection along the plane of the image. To best utilize the combined field and laboratory approach for improved interpretation of borehole EM reservoir monitoring, more frequent and earlier field images and induction logs are required. This would also provide a basis for temporal scaling between laboratory observed phenomena and observed field behavior.

ACKNOWLEDGMENT

This project was performed under the auspices of the U.S. Department of Energy through Fossil Energy research and the Office of Basic Energy Sciences by University of California Lawrence Livermore National Laboratory under Contract W-7405-Eng-48. We gratefully acknowledge past NPTO-DOE project manager Tom Reid for his support. We also acknowledge Mike Morea, Dale Julander, Qiang Zhou, Jim Copeland, and Kristin Castelucci of Chevron; Mike Hoversten and Greg Newman of Lawrence Berkeley National Laboratory; Bill Ralph, Steve Carlson, and Carl Boro of Lawrence Livermore National Laboratory for their contributions to this project.

REFERENCES

Alumbaugh, D.L., Newman, G.A., 2000, Image appraisal for 2-D and 3-D electromagnetic inversion, Geophysics, vol. 65, no. 5, p. 1455 – 1467

Bonner, B.P., J.J. Roberts, and D.J. Schneberk, Determining water content and distribution in reservoir Graywacke from the Northeast Geysers with x-ray computed tomography, Geothermal Resources Council, *Transactions*, *18*, 305–310, 1994.

Newman, G.A., and D.L. Alumbaugh, 1997, Three-dimensional massively parallel electromagnetic inversion—theory, Geophysical Journal International, 128(2), pp. 345–354

Newman, G.A., 1995, Crosswell electromagnetic inversion using integral and differential equations, Geophysics, 60(3), 899–911

Walsh, J B; Brace, W F, 1984, The effect of pressure on porosity and the transport properties of rock, Journal of Geophysical Research. B, vol.89, no.11, pp.9425-9431

Zhu, Z.Y., M.W. Haartsen, and M.N. Toksoz, Experimental studies of electrokinetic conversions in fluid-saturated borehole models, *Geophysics*, *64*(5), 1349–1356, 1999.